AEM
Journals.ASM.org

Antimicrobial Mechanism of Monocaprylate

Morten Hyldgaard,[a,b,c] Duncan S. Sutherland,[a] Maria Sundh,[a] Tina Mygind,[a,c] and Rikke Louise Meyer[a,b]

Interdisciplinary Nanoscience Center (iNANO), Aarhus University, Aarhus, Denmark[a]; Department of Bioscience, Aarhus University, Aarhus, Denmark[b]; and Danisco A/S, Brabrand, Denmark[c]

Monoglyceride esters of fatty acids occur naturally and encompass a broad spectrum of antimicrobial activity. Monocaprylate is generally regarded as safe (GRAS) and can function both as an emulsifier and as a preservative in food. However, knowledge about its mode of action is lacking. The aim of this study was therefore to elucidate the mechanism behind monocaprylate's antimicrobial effect. The cause of cell death in *Escherichia coli*, *Staphylococcus xylosus*, and *Zygosaccharomyces bailii* was investigated by examining monocaprylate's effect on cell structure, membrane integrity, and its interaction with model membranes. Changes in cell structure were visible by atomic force microscopy (AFM), and propidium iodide staining showed membrane disruption, indicating the membrane as a site of action. This indication was confirmed by measuring calcein leakage from membrane vesicles exposed to monocaprylate. AFM imaging of supported lipid bilayers visualized the integration of monocaprylate into the liquid disordered, and not the solid ordered, phase of the membrane. The integration of monocaprylate was confirmed by quartz crystal microbalance measurements, showing an abrupt increase in mass and hydration of the membrane after exposure to monocaprylate above a threshold concentration. We hypothesize that monocaprylate destabilizes membranes by increasing membrane fluidity and the number of phase boundary defects. The sensitivity of cells to monocaprylate will therefore depend on the lipid composition, fluidity, and curvature of the membrane.

The types of microorganisms that cause food poisoning are few, but they are responsible for more than one billion cases of gastrointestinal tract inflammation each year, with an estimated death toll above five million (38). Consumer demand for natural food products has amplified the importance of seeking novel preservatives to replace conventional chemicals such as nitrite, benzoate, and sorbate (38). Monoglyceride esters of fatty acids are interesting as food preservatives due to their broad spectrum of toxicity toward food-spoilage organisms *in vitro* (25, 29). In contrast to diglycerides and triglycerides, monoglycerides usually have higher antimicrobial activity than their fatty acid counterpart, and this activity is strongly affected by the type of head group (24, 25, 36). Otherwise, monoglyceride's activity depends on many of the same factors as seen for fatty acids, e.g., the length of the acyl chain and the presence, number, position, and orientation of double bonds in the chain (10, 24, 25). Monocaprylate, the monoglyceride of caprylic acid ($C_{8:0}$), is generally regarded as safe in the United States. Caprylic acid is present in coconut and babassu oil and milk fat (3). Monocaprylate is active against major food-borne pathogens like *Escherichia coli* O157:H7 (8), *Listeria monocytogenes* (33), *Streptococcus* spp., and *Yersinia* spp. (26), food-spoilage fungi such as *Penicillium* spp. and *Aspergillus* spp. (7), and herpes simplex virus (21). The mode of action for monocaprylate has not yet been investigated, and we hypothesize that it is similar to that of other monoglycerides. The amphipathic monoglycerides form micelles that penetrate the cell membrane and alter membrane permeability (4, 39). Electron microscopy studies showed that monolaurin ($C_{12:0}$) lysed *L. monocytogenes* cells and monocaprin ($C_{10:0}$) disrupted the cell membrane of *Chlamydia trachomatis* and a group B streptococcus (4, 6, 41).

Bacterial cell membranes are composed of several phospholipid species, and the ratios of the anionic phosphatidylglycerol (PG), the zwitterionic phosphatidylethanolamine (PE), and the anionic cardiolipin (CL) differ markedly between bacteria (15). In addition to these common phospholipid species, various microorganisms also contain other phospholipid species that are for example cationic, uncharged, or aminoacylated (2, 15). The distribution of phospholipids in the membrane is not random, and the properties of the membrane are therefore not uniform across the cell surface. In eukaryotes, so-called lipid rafts are nanoscale domains of tightly packed phospholipids, which are more ordered than the surrounding phospholipids. Their presence and role in the membrane's functionality are receiving increasing attention (18). In prokaryotes, the heterogeneous distribution of phospholipids in the cell membrane results in formation of domains that are considered analogous to the eukaryotic lipid rafts (16, 22). Bacterial membranes encompass a solid ordered (S_o) lipid phase enriched in CL and a liquid disordered (L_d) lipid phase (13, 14, 23, 35). Using the CL-binding stain 10-*N*-nonyl acridine orange (NAO) on *E. coli* "minicells" that are mainly composed of phospholipids found at the cell poles, it was documented that CL-containing domains form at the poles and septum of rod-shaped bacteria, and that these are important for several cellular functions (22, 27, 31). These domains thus appear to be important for the properties and functionality of prokaryotic membranes.

In the present study, we use *E. coli*, *Staphylococcus xylosus*, and *Zygosaccharomyces bailii* as model organisms to investigate the mode of action of monocaprylate. The Gram-negative *E. coli* is a common pathogen problem in the food industry and is a major public health concern (33). *S. xylosus* is a nonpathogenic Gram-positive bacterium isolated from human skin and can be found in naturally fermented sausages or it can be added as a starter culture (11). The yeast *Z. bailii* is a major food-spoilage organism in, e.g.,

Received 15 October 2011 **Accepted** 6 February 2012
Published ahead of print 17 February 2012
Address correspondence to Rikke Louise Meyer, rikke.meyer@inano.au.dk.
Supplemental material for this article may be found at http://aem.asm.org/.

doi:10.1128/AEM.07224-11

mayonnaise and beverages, and known acid- and preservative-resistant yeast (17). The mode of action of monocaprylate was investigated by examining its effect on the survival, structure, and membrane permeability of microbial cells and by studying its interaction with and incorporation into model membranes prepared as vesicles or supported lipid bilayers.

MATERIALS AND METHODS

Materials. *S. xylosus* (DSM 20266), *E. coli* K-12 (DSM 498), and *Z. bailii* (DSM 70492) were used as model organisms. Propidium iodide (PI) powder was acquired from Invitrogen Molecular Probes (OR). Calcein disodium salt and Triton X-100 were obtained from Fluka (Buchs, Switzerland). Lipids were purchased from Avanti Polar Lipids (Alabaster, AL). Yeast polar lipid extract (*Saccharomyces cerevisiae*, 190001C), CL (*E. coli*, 841199C), PE (*E. coli*, 840027C), and PG (*E. coli*, 841188C) were provided in chloroform, whereas *E. coli* total lipid extract (57.5% PE, 15.1% PG, 9.8% CL, and 17.6% others) and *E. coli* polar lipid extracts (67% PE, 23.2% PG, and 9.8% CL) were purchased as powders. Monocaprylate had a minimum monoglyceride content of 85% and was provided by Danisco A/S (Brabrand, Denmark). Monocaprylate was suspended in MOPS (morpholinepropanesulfonic acid) buffer at 35°C and stirred until fully dissolved before it was sterile filtered (0.2 μm, Q-Max syringe filter; Frisenette ApS, Knebel, Denmark) into a sterile Falcon tube. We calculated all concentrations as if monocaprylate had 100% monoglyceride content with no diglycerides or triglycerides present.

Cell cultures. *E. coli* and *S. xylosus* were cultured overnight at 30°C and 120 rpm shaking in 8 g/liter nutrient broth or 30 g/liter tryptic soy broth, respectively. *Z. bailii* was grown for 48 h in DSMZ medium 186 (3 g/liter yeast extract, 3 g/liter malt extract, 5 g/liter peptone, 10 g/liter glucose) at 25°C and 100 rpm shaking.

Optical antimicrobial activity assay. The MIC for monocaprylate was determined by monitoring cell growth in a flat-bottomed 96-well microtiter plate (no. 3596, Costar; Corning Incorporated, NY) with monocaprylate concentrations ranging from 0 to 10 mM. Microorganisms for inoculation of the microtiter plate were grown in liquid media and harvested in the mid-log growth phase by centrifugation (5,000 $\times$ *g*, 10 min). Cells were resuspended in growth media to a final optical density at 600 nm (OD_{600}) = 0.005. Wells were inoculated with 200 μl culture. Cell-free controls were inoculated with the same volume of sterile media. Monocaprylate in MOPS was added from a 50-mM sterile filtered stock solution to obtain final concentrations ranging from 0 to 10 mM. Four replicate wells were prepared for each monocaprylate concentration. An OD_{562} was monitored before and after overnight incubation at 30°C (25°C for yeast) using a plate reader (ELx800; Bio-Tek Instruments Inc., VT). The OD_{562} of cell-free wells containing the same monocaprylate concentration was subtracted from sample wells to account for absorbance by monocaprylate. MIC was defined as the lowest monocaprylate concentration resulting in an increase in the $OD_{562} \leq 20\%$ of the value obtained from cells grown without monocaprylate.

Assessment of cell viability. MIC tests only address the inhibition of cell growth and do not provide information about cell viability. Viability of monocaprylate-treated cells was measured by counting CFU after exposing cells suspended in MOPS buffer to monocaprylate.

The following was performed at 20°C for all microorganisms, except *E. coli*, where 15°C and 37°C also were included. Cell suspensions (harvested in mid-log growth phase and resuspended to OD_{600} = 0.05 in MOPS) were distributed in 33 1-ml aliquots in sterile Eppendorf tubes. Sterile filtered monocaprylate in MOPS was then added to a final concentration ranging from 0 to 10 mM in triplicate. Samples were vortexed and incubated 1 h. Each sample was then 10-fold serially diluted, and 100 μl was spread plated onto agar plates. CFU were counted after incubation for 24 h at 30°C (48 h at 25°C for *Z. bailii*).

AFM imaging of cell structure. We used atomic force microscopy (AFM) to examine the monocaprylate effect on the microorganism cell structure over time. Cells were immobilized to 18-mm circular coverslips by coating these with Cell-TAK (Becton Dickinson Biosciences, Temse, Belgium) as described in reference 30. Cells were harvested in the mid-log growth phase and resuspended in MOPS buffer (OD_{600} = 0.2, except 0.1 for yeast), and a drop of cell suspension was placed on the Cell-TAK-coated coverslip and incubated for 15 min before rinsing vigorously with Milli-Q water. The coverslip with immobilized cells was then submerged in MOPS with or without monocaprylate at 2$\times$ MIC for 60 or 240 min. We defined 2$\times$ MIC to be 20.4 mM for *E. coli*, 18 mM for *S. xylosus*, and 8 mM for *Z. bailii.*

After incubation with monocaprylate, the coverslips were rinsed with Milli-Q water and air dried. AFM images were recorded with a JPK NanoWizard II AFM (JPK Instruments, Berlin, Germany) at 512 pixels per line, at a scan rate of 0.5 Hz. Cells were imaged in intermittent contact mode in air using Si_3N_4 cantilevers (OMCL-AC160TS; Olympus, Mannheim, Germany). Cantilevers had a resonance frequency of 300 kHz and a spring constant of 42 N/m. Images of at least three cells were recorded from one sample.

Assessing the cell membrane integrity with fluorescence microscopy. Gelatin-coated coverslips were used to immobilize cells for fluorescence microscopy as described in reference 32. Cells were harvested in the mid-log growth phase and resuspended in MOPS buffer (OD_{600} = 0.4, except 0.2 for yeast). PI staining was used to evaluate the cell membrane integrity during exposure to monocaprylate. We added 200 μl MOPS and 50 μl 0.03 mM PI to the immobilized cells and incubated them in the dark for 15 min before imaging with a Zeiss Axiovert 200 M epifluorescence microscope (Zeiss, Göttingen, Germany). Phase-contrast images and fluorescence images (using Zeiss filter set 43) were combined to visualize all cells while identifying cells that had taken up PI. A time series of images of the same field of view were taken sequentially every 3 min before and after addition of monocaprylate to 2$\times$ MIC. All analyses were performed on triplicate samples.

Assessing the interaction between model membranes and monocaprylate. (i) Preparing small unilamellar vesicles (SUVs) for generation of supported lipid membranes. Two natural lipid extracts were used to form supported lipid bilayers (SLBs): *E. coli* polar lipid extract, representing Gram-negative bacterial membranes, and *S. cerevisiae* polar lipid extract, representing yeast membranes. Polar lipid extracts were used in this experiment because the lipid composition is better characterized than for total lipid extracts, in which 17.6% of the content is unaccounted for. Furthermore, the use of polar lipid extracts enabled us to compare results from experiments on natural lipid extracts with results from experiments on blends of purified natural lipids. The role of CL in interacting with monocaprylate was investigated by studying SLBs made from combinations of the pure lipids PE, PG, and CL in combinations providing either CL-deficient (PE/PG/CL = 62:18:0) or high-CL (PE/PG/CL = 72:28:20) membranes.

The lipid powder was dissolved in a round-bottomed flask in 1:1 (vol/vol) chloroform and methanol, while lipid solution was used as provided. The organic solvent was evaporated under a nitrogen stream, and the resulting lipid film was dried in a desiccator under vacuum for 2 h. Multilamellar vesicles (MLVs) were obtained by hydrating the lipid film in MOPS to a final concentration of 10 mg lipid/ml. The lipid solution was sparged with nitrogen gas to prevent oxidation of the lipids. The MLV solution was kept overnight at 37°C (45°C for yeast lipids) at 100 rpm shaking. The lipid solution was frozen and thawed 10 times by alternating between liquid N_2 and a 40°C (45°C for yeast lipids) water bath to obtain unilamellar vesicles (ULVs). We sonicated the ULV solution for 30 min in an ice bath using a rod sonicator (70 W, 50% of maximal power, 3-mm probe diameter, Sonopuls ultrasonic homogenizers; Bandelin Electronic, Berlin, Germany) to obtain small unilamellar vesicles (SUVs). The SUV solution was sterile filtered through a 0.2-μm Q-Max cellulose-acetate filter to remove titanium particles from the rod sonicator.

(ii) Membrane permeability measured by calcein dye release. A vesicle model experiment was performed to assess monocaprylate's direct interaction with a membrane. Calcein self-quenches at high concentra-

tions and fluoresces when diluted. Calcein was used as an indicator for membrane permeabilization by monitoring changes in fluorescence intensity due to leakage from vesicles.

Calcein-loaded vesicles were prepared from *E. coli* total lipid extracts using the same procedure as described above, except that the MOPS buffer contained 70 mM calcein. We used the *E. coli* total lipid extract in the initial model membrane assay in order to work with membranes that resemble the natural membrane of cells. In replacement of sonication, the vesicle suspension was extruded 15 times through a Nuclepore track-etched membrane with a pore size of 100 nm (Whatman, Clifton, NJ) using a MiniExtruder with a heating block (Avanti Polar Lipids, Alabaster, AL) at 40°C to obtain large unilamellar vesicles (LUVs). The calcein-LUV solution was loaded on a PD-10 desalting column (GE Healthcare, Buckinghamshire, United Kingdom), previously equilibrated in MOPS, to remove free calcein. Eluted aliquots of 0.5 ml were collected and the calcein-LUV-containing fractions were pooled and diluted in MOPS to a lipid concentration of approximately 3 μM. Membrane permeabilization was followed by monitoring the release of entrapped calcein into the buffer at 20°C using a thermostated Varian Cary Eclipse spectrofluorometer (Varian, Palo Alto, CA). Calcein was excited at 480 nm, and emission was monitored at 520 nm using 5-nm slits and medium photomultiplier tube (PMT) voltage. The baseline intensity (F_0) was recorded of a 750-μl calcein-LUV suspension in a quartz cuvette containing a magnet (Hellma, Müllheim, Germany). We added 10 μl monocaprylate and monitored calcein release as changes in intensity (F_{sample}). Subsequent addition of 10 μl 2% Triton X-100 yielded the maximum calcein release (F_{max}) due to complete vesicle disruption. The percentage of leaked calcein was calculated by the following equation:

$$\text{calcein leakage} = \frac{(F_{sample} - F_0)}{(F_{max} - F_0)} \times 100\%$$

(iii) Assessing the binding of monocaprylate to SLBs. We hypothesized that monocaprylate interacted with the lipid bilayer and therefore monitored changes in mass and viscoelastic properties during monocaprylate exposure. These parameters were measured by quartz crystal microbalance with dissipation (QCM-D), where changes in the resonance frequency and dissipation of an oscillating quartz crystal indicate changes in mass and viscoelastic properties of the membrane.

A 10-nm layer of Ti was deposited (on a homebuilt electron beam-stimulated thermal evaporation system) onto an Au-coated quartz crystal sensor (5 MHz, Q-Sense AB, Sweden), followed by a similar deposition of a 30-nm layer of SiO_2. The sensor crystals were stored in 2% SDS, washed with Milli-Q water, dried in a stream of nitrogen gas, and subjected to UV-ozone treatment for 40 min. UV-treated sensor crystals were washed with Milli-Q water and dried in a stream of nitrogen gas before mounting in the QCM-D mounting chambers. Measurements were performed with the Q-Sense E4 system (Q-Sense AB, Sweden) thermostabilized at 22°C. We monitored each sensor crystal using the Q-soft software (version 2.5.6.494) at the 3rd, 5th, 7th, 9th, and 11th overtones of the fundamental resonance frequency.

SLBs were formed by introducing MOPS with 0.3 mg/ml SUV lipid solution and 20 mM $CaCl_2$, at a flow rate of 0.1 ml/min using an Ismatec IPC-N 4 peristaltic pump (Ismatec SA, Glattburg, Switzerland). MOPS without $CaCl_2$ was flushed through to remove excess lipid, and monocaprylate dissolved in MOPS was then injected in increasing concentrations and finally replaced by MOPS. Changes in frequency and dissipation refer to measurements of the 5th harmonics and were normalized to the fundamental frequency by dividing with 5. We collected data from three crystals for *E. coli* and *Saccharomyces cerevisiae*. Data modeling of two raw data sets of *E. coli* lipid membranes for SLB thickness and viscosity using the one-layer Voigt viscoelastic model was performed in QTools (Q-Sense AB, Sweden). Modeling data for one of the three *E. coli* data sets were not included because of negative dissipation after formation of a stable membrane. Data from the 5th and 7th harmonics were fitted to the Voigt model. We used fixed parameters for the fluid density (1,000 kg/m^3), the fluid viscosity (0.001 Pa · s), and the layer density (1,100 kg/m^3). We fitted the layer parameters within the following boundaries: viscosity (0.0006 to 0.01 Pa · s), shear (500 to 1×10^9 Pa), and thickness (1×10^{-10} to 1×10^{-7} m).

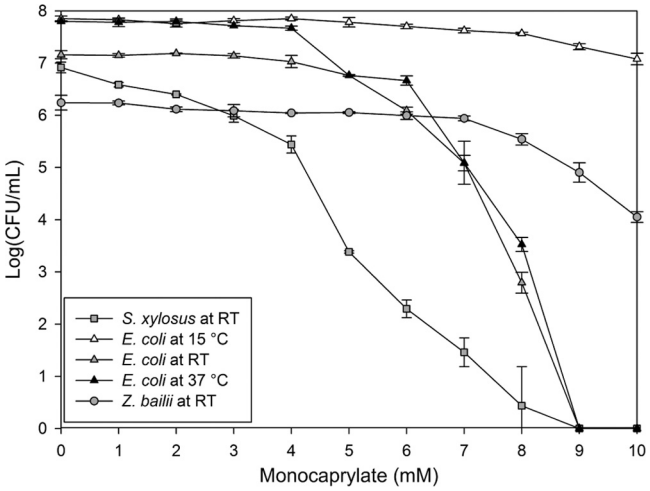

FIG 1 Number of viable *S. xylosus* (□), *E. coli* (△), and *Z. bailii* (○) cells after 1 h exposure to monocaprylate at room temperature (gray) but also 15°C (white) and 37°C (black) for *E. coli*. Error bars = standard deviations (SD) ($n = 3$).

(iv) Supported lipid bilayer topographic response to monocaprylate treatment. We visualized the integration of monocaprylate into SLBs by AFM. Membranes were formed on mica by adding an SUV solution (prepared as described above) with 20 mM $CaCl_2$ and 0.3 mg lipid/ml in MOPS to freshly cleaved mica and incubating for 20 min before washing with MOPS. AFM imaging was performed by contact mode imaging in MOPS (with or without monocaprylate) using a NanoWizardII AFM (JPK Instruments) and Si_3N_4 cantilevers (NP and CSC38/noAl; Veeco, CA, and Mikromasch, Tallinn, Estonia, respectively) with a nominal spring constant of 0.03 to 0.09 N/m.

RESULTS

Antimicrobial effect of monocaprylate. We assessed monocaprylate's antimicrobial activity by monitoring its inhibitory effect on growth and viability of the three model organisms. Monocaprylate inhibited the growth of *E. coli* at 8 mM, *S. xylosus* at 9 mM, and *Z. bailii* at 4 mM. Cell viability was also affected, and the 50% lethal concentration (LC_{50}) was 5 mM, 1 mM, and 7 mM for *E. coli*, *S. xylosus*, and *Z. bailii*, respectively (Fig. 1). The effect of monocaprylate was temperature dependent. Increasing the temperature from room temperature to 37°C led to a stronger antibacterial effect at a similar monocaprylate concentration and incubation period. Furthermore, decreasing the temperature to 15°C lowered the antimicrobial effect of monocaprylate. LC_{50} at 15°C was 8 mM, and the number of viable cells had only decreased by one log unit even at 10 mM monocaprylate (Fig. 1).

Effect of monocaprylate on cell morphology and membrane integrity. We then investigated monocaprylate's effect on cell structure and membrane integrity using AFM and fluorescence microscopy. Treatment with monocaprylate at 2× MIC resulted in the appearance of small indentations in *E. coli* cells, which were not observed in untreated cells (Fig. 2A to C). No effects were seen on *S. xylosus* cells after 60 min of exposure, but indentations appeared after 240 min (Fig. 2D to F). We observed a rougher surface of *Z. bailii* cells after 60 min of monocaprylate treatment (Fig. 2H),

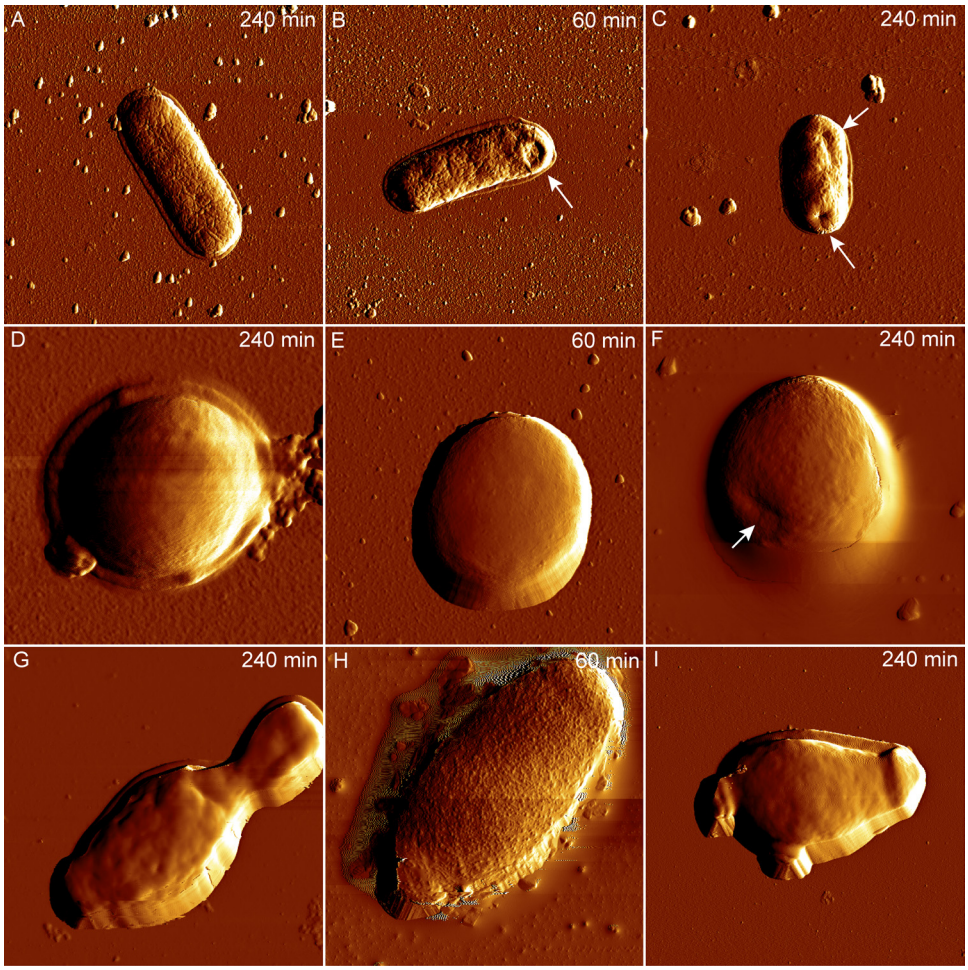

FIG 2 AFM amplitude images of *E. coli* (A to C), *S. xylosus* (D to F), and *Z. bailii* (G to I) cells recorded in air after exposure to monocaprylate. The untreated cells (A, D, G) were incubated 240 min in MOPS. Cells treated with 20.4 mM (B and C), 18 mM (E and F), or 8 mM (H and I) monocaprylate for 60 min (B, E, and H) or 240 min (C, F, and I). White arrows indicate visible changes in cell structure. Images of *E. coli*, *S. xylosus*, and *Z. bailii* were 5 by 5 μm, 2 by 2 μm, and 10 by 10 μm, respectively.

but because these structures were not observed on samples that had been exposed 240 min, these structures may be an artifact from sample handling. Untreated and treated yeast cells after 240 min of incubation had no structural differences (Fig. 2G and I).

Although effects on the cell structure were not apparent for all the microorganisms tested, they all took up PI within seconds of monocaprylate exposure, indicating that the cell membrane was compromised (Fig. 3). In *Z. bailii*, the PI stain was initially constricted to the nuclei, but within 2 min of exposure, the nuclei shrank and the PI stain spread to the entire cell, indicating that the nuclear envelope had dissolved, releasing DNA to the cytoplasm (Fig. 3F; see also Video S1 in the supplemental material).

Interaction of monocaprylate with lipid bilayers. The immediate membrane permeabilization indicated that monocaprylate acted on the cell membrane, and we therefore used two model systems to specifically study the interaction of monocaprylate with a phospholipid bilayer. In the first model system, membrane permeabilization was measured using calcein-loaded 100-nm unilamellar vesicles. These vesicles contained no membrane proteins and represented the phospholipid bilayer of *E. coli* cells. Permeabilization of the vesicles occurred at approximately 1 mM monocaprylate, corresponding to a monocaprylate/lipid ratio of 420:1 (Fig. 4). The permeabilization only resulted in 28% calcein release compared to dissolving the vesicles in Triton X (Fig. 4), and increasing the monocaprylate concentration further did not increase the release beyond 39%. We could not increase the monocaprylate concentration beyond 5 mM in the experiment because higher levels of monocaprylate caused dispersion of the light beam, resulting in obstruction of the measurements.

In the second model system, we prepared SLBs on substrate surfaces. We used two natural lipid extracts to represent the cell membranes of Gram-negative bacteria and yeast. The main difference of these membranes is their phospholipid profile, where *E. coli* lipid extract has three phospholipid-species (PE, PG, and CL) comprising 100% of the phospholipids, while yeast lipid extract has nine phospholipid species (phosphatidylcholine, phosphatidylinositol, phosphatidylserine, PE, lyso-PE, phosphatidic acid, lysophosphatidylcholine, PG, and glycerophosphatidylcholine [listed in order of abundance]) comprising 80% of the phospholipids. Interaction of monocaprylate with the bilayer was investigated by monitoring changes in resonance frequency (Δf) and dissipation (ΔD) by the QCM-D technique.

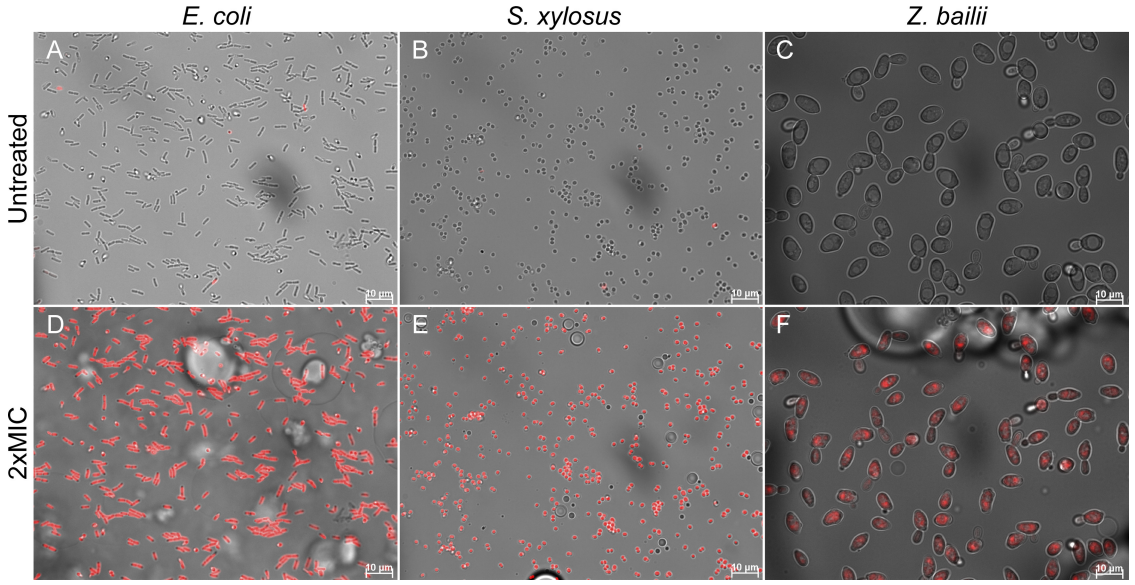

FIG 3 Overlay of bright field and fluorescence images of cells in MOPS with PI, before (A, B, and C) and 6 min after addition of monocaprylate at 20.4 mM (D), 18 mM (E), and 8 mM (F). Cells with compromised membranes are stained with PI (red). Monocaprylate bubbles are visible in treated samples.

E. coli lipid SLB formed on the quartz crystal by adsorption of vesicles onto the substrate and subsequent vesicle rupture during $CaCl_2$-free MOPS buffer rinsing (Fig. 5A). The formation of SLB occurred in a similar manner as previously reported for other lipid compositions (40). The resulting membrane gave a resonance frequency shift of -27.1 ± 0.9 Hz and a concomitant dissipation change of $(0.44 \pm 0.5) \times 10^{-6}$ (Fig. 5A), indicating a good-quality bilayer across the surface. Addition of monocaprylate up to 2.5 mM had no noticeable effect on the frequency shift and only a slight effect on the dissipation induced by the layer. However, exposure to 5 mM monocaprylate (equivalent of LC_{50}) resulted in an abrupt and irreversible increase in frequency ($\Delta f = -8.9 \pm 1.3$ Hz) and dissipation of the bilayer ($\Delta D = [+2.4 \pm 0.5] \times 10^{-6}$) (white circles, Fig. 5A). Data modeling suggested that the *E. coli* lipid bilayer mass increased 2 to 4 times with a concomitant increase in thickness, and the viscosity decreased below that of a rigid untreated SLB after monocaprylate treatment (see Fig. S1 in the supplemental material). Taken together, the results suggest that the bilayer becomes more hydrated and floppy after treatment with monocaprylate. The bilayer properties were largely maintained after rinsing, indicating that the changes implemented by the monocaprylate treatment are stable.

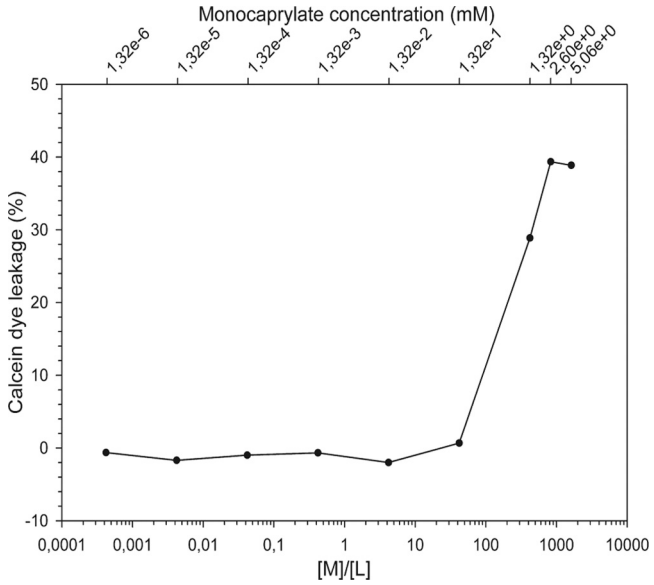

FIG 4 *E. coli* membrane permeabilization by monocaprylate monitored by leakage of calcein dye from vesicles as a function of the monocaprylate to lipid concentration ([M]/[L]) ratio. At each [M]/[L] ratio, the intensity signal from the released calcein was normalized to the signal obtained at complete vesicle rupture. The monocaprylate concentration used at each measured [M]/[L] ratio is given at the upper axis. A lipid concentration [L] of ~3 μM was used for all [M]/[L] ratios.

S. cerevisiae SLB formed by spontaneous vesicle rupture. The QCM profile during the SLB formation differed from *E. coli* SLB by containing a second phase of adsorption before rinsing with MOPS. Such a phase has previously been linked to adsorption of intact vesicles onto the membrane surface for complex lipid compositions (40). The process showed a significant baseline drift of frequency and dissipation over time (0 to 15 min, Fig. 5B), and the data were therefore only analyzed semiquantitatively by comparing trends in Δf and ΔD with no relation to their absolute values. Formation of *S. cerevisiae* lipid SLBs resulted in a resonance frequency shift of -31.5 ± 1.5 Hz and a concomitant change in dissipation of $(2.7 \pm 0.2) \times 10^{-6}$ (Fig. 5B). These values are in the range for bilayer formation but show a relatively high dissipation likely from a small fraction of intact vesicles remaining. Previous studies have shown significant differences in the ease of vesicle rupture dependent on lipid composition (37). Low concentrations of monocaprylate affected resonance frequency and dissipation, signifying that monocaprylate adsorbed to or integrated into the SLB (white triangle, Fig. 5B). Monocaprylate treatment increased bilayer frequency ($\Delta f = -2 \pm 2.6$ Hz) and dissipation ($\Delta D = [+1.4 \pm 0.1] \times 10^{-6}$) compared to the untreated SLB (Fig. 5B), which indicates an increase in the mass and likely the hydra-

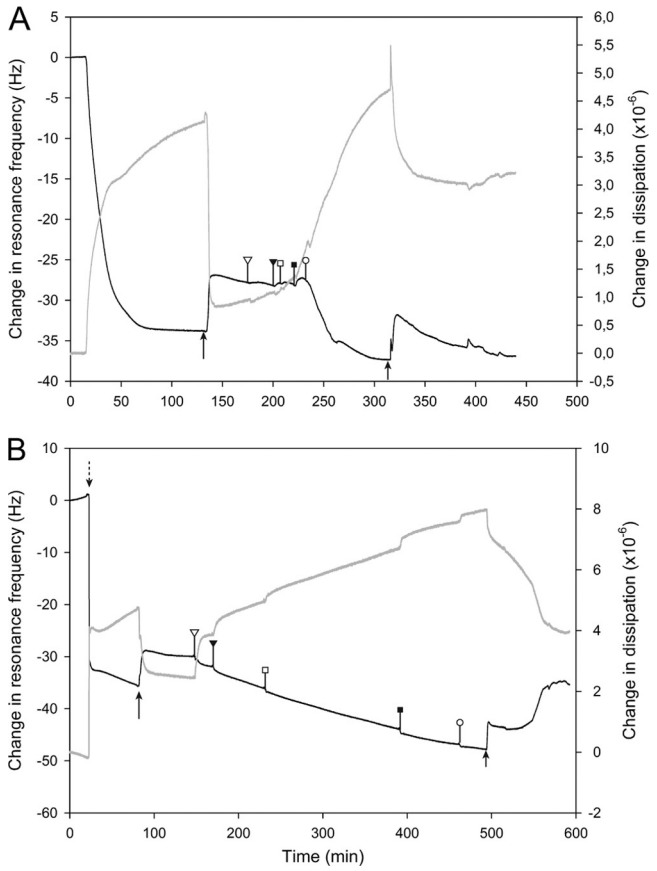

FIG 5 Interaction of monocaprylate with an SLB as observed by QCM-D. Measurement of dissipation (gray line) and frequency (black line) changes at the 5th harmonic of *E. coli* and *S. cerevisiae* membranes are shown. To form SLBs, we injected a lipid vesicle solution with 20 mM $CaCl_2$ into the QCM-D chambers (dotted arrow). All rinsing steps were performed with $CaCl_2$-free MOPS buffer (black arrows). (A) *E. coli* lipid membrane treated with monocaprylate in a final concentration of 0.05 mM (white triangle), 0.25 mM (black triangle), 0.5 mM (white square), 2.5 mM (black square), and 5 mM (white circle) before rinsing. (B) For the *S. cerevisiae* lipid membrane, monocaprylate was injected at concentrations equal to 1 mM (white triangle), 2 mM (black triangle), 3 mM (white square), 4 mM (black square), and 5 mM (white circle) before rinsing.

tion of the layer. The dynamics observed in the changes in resonance frequency and dissipation observed during rinsing with MOPS after monocaprylate exposure suggest the following: the sudden drop in mass (increase in resonance frequency) and dissipation at the onset of rinsing (small arrow, Fig. 5B) indicates that the addition of mass during monocaprylate exposure was reversible. This immediate loss of material with a concomitant loss of dissipation may indicate that the material adsorbed was present as micelles, allowing rapid desorption of a large fraction of the monocaprylate. Subsequently (at 500 to 540 min), the dissipation changed gradually without any change in resonance frequency, suggesting reorganization of the bilayer. Finally (at 540 to 575 min), changes in the resonance frequency indicated further loss of mass with a lower rate (Fig. 5B). Monocaprylate's interaction with the yeast membrane thus differed from that with the bacterial membrane because the membrane rearranged, and monocaprylate was removed during rinsing with MOPS.

All results pointed to the cell membrane as the site of action. Indeed, imaging of SLBs made from *E. coli* lipids revealed the appearance of nanoscale domains approximately 2 to 2.5 nm taller than the SLB, after exposure to monocaprylate (Fig. 6). The *E. coli* SLBs were composed of two phases: a 3.5-nm-tall L_d phase and 0.4- $\pm$ 0.1-nm-tall S_o phase (Fig. 6A). The 6-nm-tall nanoscale domains only appeared in the L_d phase and only after exposure to monocaprylate (light areas in Fig. 6E and I), and we suggest that the nanoscale domains are monocaprylate interacting with the surface of the bilayer or integrating into the bilayer. Monocaprylate melts at 35°C and should therefore be a stable but adhesive substance at room temperature. Lateral deflection images provide information about the friction forces between the AFM tip and the sample, and contrast in these images revealed that the nanoscale domains were highly adhesive, supporting that these were indeed monocaprylate (Fig. 6E and I, insets).

Yeast SLBs consisted mainly of the L_d phase (Fig. 6B). Exposure to monocaprylate resulted in appearance of nanoscale domains, as was observed for *E. coli* SLBs (cross sections, Fig. 6F and J), and integration of monocaprylate into the yeast SLB was also indicated by the appearance of areas that were slightly higher (0.2 nm) and much more adhesive than the untreated SLB (Fig. 6B, F, and J).

We hypothesized that monocaprylate's interaction with the membrane involves free CL in the L_d phase because CL is known to form domains in lipid membranes (12, 14). We therefore tested the effect on SLBs made from combinations of pure phospholipids (PE and PG) with or without CL. The lipid composition of the SLB with CL was similar to that of *E. coli* membranes, but with twice the amount of CL, and therefore termed "high-CL." The high-CL SLB contained both L_d and S_o phases, while CL-deficient SLBs contained only the L_d phase (Fig. 6C and D). The result for monocaprylate treatment of the CL-deficient SLB was similar to what was observed for yeast SLB: integration of monocaprylate in the membrane was barely visible in the height image but was easily revealed by areas of high friction in the lateral deflection image (Fig. 6G and K). Treatment of the high-CL SLB resulted in partial desorption of the SLB. Interestingly, the remaining membrane had no nanoscale domains (Fig. 6H and L). Taken together, these results suggest that monocaprylate integrates in the L_d phase of the membrane and that the presence of CL is not required for its interaction with the bilayer (Fig. 6).

DISCUSSION

The antimicrobial effect of monocaprylate. We found a similar antimicrobial effect of monocaprylate on Gram-positive and Gram-negative bacteria, and MIC values were in the range of what has been found previously (26, 34). In contrast to our findings, Kollanoor et al. (26) observed that Gram-negative bacteria were less susceptible than Gram-positive bacteria, although the susceptibility was species specific and the MIC varied from 5 to 20 mM. The susceptibility of yeast and fungi is also species specific. While we found a MIC of 4 mM for *Z. bailii*, previous studies have documented MIC values ranging from 0.15 to 10 mM for a wide range of yeast and fungi (5, 7). Interestingly, the MIC of bacteria was similar to the concentration for which no viable cells were detected, and growth inhibition was thus directly linked to loss of viability (Fig. 1). In contrast, the growth of *Z. bailii* was inhibited even below the LC_{50}, indicating that monocaprylate could affect cell growth at low concentrations without affecting cell viability noticeably.

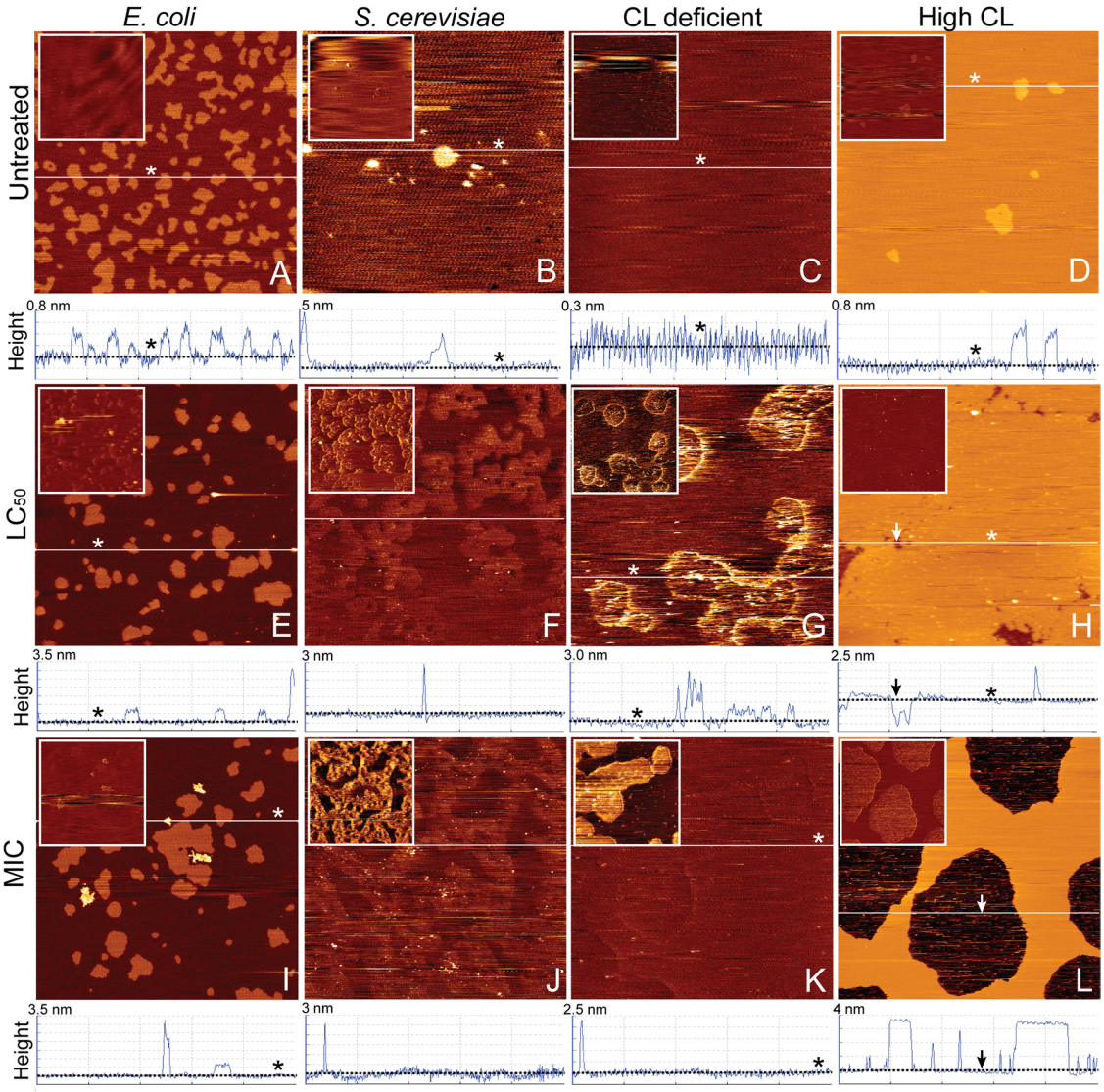

FIG 6 Contact mode AFM height images of monocaprylate's effect on SLBs from *E. coli* and *S. cerevisiae* recorded in MOPS. Representative images of untreated SLBs of *E. coli* lipid (9.8% CL) (A), *S. cerevisiae* lipid (B), *E. coli* lipid without cardiolipin (C), and *E. coli* lipid with high cardiolipin content (20% CL) (D). Untreated SLBs were exposed to monocaprylate for an hour at a final concentration corresponding to LC_{50} (5 mM [E, G, H], 7 mM [F]) and MIC (10.2 mM [I, K, L], 4 mM [J]). The SLBs were rinsed with MOPS before imaging. Below each height image is a cross-sectional profile taken at the white line in the corresponding images. The liquid disordered lipid phase and holes are illustrated with asterisks and arrows, respectively. In the 5- by 5-μm height images, the lighter areas correspond to higher structures. The insets are vertical deflection images of the same area as the corresponding height image; lighter areas correspond to higher lateral friction between tip and sample.

Monocaprylate integrates into the membrane's L_d phase and destabilizes it. We expected monocaprylate's site of action to be the cell membrane, as monoglycerides are generally proposed to act as nonionic surfactants that interact with and disrupt membranes (4, 6, 39). In theory, integration of monocaprylate in the membrane would lower the membrane's melting temperature (19, 28) and thereby increase its fluidity and permeability (9). We therefore hypothesized that monocaprylate integrates into the membrane and destabilizes it, which results in membrane permeabilization. Indeed, we show that monocaprylate was incorporated into the L_d phase of the membrane (Fig. 6), made it more hydrated (Fig. 5), and caused permeabilization of the membrane (Fig. 3 and 4). AFM images indicated that monocaprylate incorporated as nanoscale domains in the *E. coli* and high-CL SLB, while it caused phase separation of the CL-deficient and yeast SLB. The phase boundaries may play a role in membrane permeabilization. The interface between two lipid phases has a line tension that induces packing defects at the hydrophobic interface of lipid phases, and these defects increase membrane permeability (1, 9, 16). We therefore propose that monocaprylate also destabilizes the membrane by increasing the number of phase boundary defects.

We observed one noticeable discrepancy between experiments with microbial cells and with model membrane systems: the membrane vesicles made from *E. coli* lipids were permeabilized at concentrations much below the MIC of *E. coli* cells (Fig. 1 and 4). Two

important differences between the two experiments are the strong curvature and the absence of proteins in the 100-nm vesicles. Knowing that monocaprylate integrates into the lipid bilayer, our results indicate the membrane curvature also affects its susceptibility toward monocaprylate. Monocaprylate is, like all alkyl chains, a sensor of membrane curvature (20). Highly curved membranes have more defects that expose the hydrophobic bilayer core and therefore will recruit larger densities of amphiphilic molecules (20). The reason we did not see higher calcein release from vesicles could be because monocaprylate either caused transient disruption of the calcein-loaded vesicles or induced calcein release in a concentration-independent manner. The latter explanation suggests that monocaprylate affects membranes in an "all or nothing" mechanism, where some vesicles are permeabilized while others are not. However, a conclusive statement about the cause of the low calcein release from vesicles cannot be made without further investigations.

Monocaprylate did not incorporate randomly into the membrane, and there were visible differences in how monocaprylate integrated into membranes with different phospholipid compositions (Fig. 6). The large variability in susceptibility observed among different microorganisms may thus be linked to differences in phospholipid composition and membrane fluidity. Temperature may therefore also play an important role for the antimicrobial activity of monocaprylate. Lowering the temperature would increase the ratio of S_o to L_d phases in the membrane (23), potentially leading to lower susceptibility to incorporation of monocaprylate. With this in mind, we examined the susceptibility of *E. coli* toward monocaprylate at different temperatures. As expected, *E. coli* was much less susceptible when lowering the temperature to 15°C. It should be noted that the solubility of monocaprylate may also be affected by the lower temperature, resulting in lower availability of monocaprylate, which might also contribute to the lower antimicrobial effect. It is, nevertheless, interesting to note that the antimicrobial properties of monocaprylate are temperature dependent, especially at temperatures below room temperature.

In summary, monocaprylate's mode of action somewhat resembles that of free fatty acids or surfactants, which form transient or permanent pores in the membrane or even solubilize membranes (10). The observation that monocaprylate only integrates into the L_d phase of the membrane indicates that membrane fluidity and phospholipid composition are key factors in determining an organism's susceptibility. The significance of these parameters might explain the large variation in susceptibility to monocaprylate among different species of bacteria, yeast, and fungi. Furthermore, environmental parameters that influence membrane fluidity should be considered if using monocaprylate as a food preservative.

ACKNOWLEDGMENTS

We thank Søren B. Nielsen for assistance with and use of the spectrofluorometer and Brian Vad for his introduction into atomic force microscopy of supported lipid bilayers. We thank the Carlsberg Foundation for their support for Rikke Louise Meyer.

REFERENCES

1. **Arouri A, Dathe M, Blume A.** 2009. Peptide induced demixing in PG/PE lipid mixtures: a mechanism for the specificity of antimicrobial peptides towards bacterial membranes? Biochim. Biophys. Acta **1788**:650–659.
2. **Arthur H, Watson K.** 1976. Thermal adaptation in yeast: growth temperatures, membrane lipid, and cytochrome composition of psychrophilic, mesophilic, and thermophilic yeasts. J. Bacteriol. **128**:56–68.
3. **Beare-Rogers J, Dieffenbacher A, Holm JV.** 2001. Lexicon of lipid nutrition. Pure Appl. Chem. **73**:685–744.
4. **Bergsson G, Arnfinnsson J, Karlsson SM, Steingrímsson O, Thormar H.** 1998. *In vitro* inactivation of *Chlamydia trachomatis* by fatty acids and monoglycerides. Antimicrob. Agents Chemother. **42**:2290–2294.
5. **Bergsson G, Arnfinnsson J, Steingrímsson O, Thormar H.** 2001. *In vitro* killing of *Candida albicans* by fatty acids and monoglycerides. Antimicrob. Agents Chemother. **45**:3209–3212.
6. **Bergsson G, Arnfinnsson J, Steingrímsson O, Thormar H.** 2001. Killing of Gram-positive cocci by fatty acids and monoglycerides. APMIS **109**: 670–678.
7. **Bunková L, et al.** 2010. Influence of monoacylglycerols on growth inhibition of micromycetes *in vitro* and on bread. Eur. J. Lipid Sci. Technol. **112**:173–179.
8. **Chang SS, Redondo-Solano M, Thippareddi H.** 2010. Inactivation of *Escherichia coli* O157:H7 and *Salmonella* spp. on alfalfa seeds by caprylic acid and monocaprylin. Int. J. Food Microbiol. **144**:141–146.
9. **Cullis PR, Hope MJ.** 1985. Physical properties and functional roles of lipids in membranes, p 25–72. *In* Vance DE, Vance JE (ed), Biochemistry of lipids and membranes. Benjamin/Cummings Publishing Company, Menlo Park, CA.
10. **Desbois AP, Smith VJ.** 2010. Antibacterial free fatty acids: Activities, mechanisms of action and biotechnological potential. Appl. Microbiol. Biotechnol. **85**:1629–1642.
11. **Di Maria S, Basso AL, Santoro E, Grazia L, Coppola R.** 2002. Monitoring of *Staphylococcus xylosus* DSM 20266 added as starter during fermentation and ripening of soppressata molisana, a typical Italian sausage. J. Appl. Microbiol. **92**:158–164.
12. **Doménech Ò, et al.** 2009. Interactions of oritavancin, a new lipoglycopeptide derived from vancomycin, with phospholipid bilayers: effect on membrane permeability and nanoscale lipid membrane organization. Biochim. Biophys. Acta **1788**:1832–1840.
13. **Doménech Ò, Merino-Montero S, Montero MT, Hernández-Borrell J.** 2006. Surface planar bilayers of phospholipids used in protein membrane reconstitution: an atomic force microscopy study. Colloids Surf. B Biointerfaces **47**:102–106.
14. **Domènech Ò, Morros A, Cabañas ME, Montero MT, Hernández-Borrell J.** 2007. Thermal response of domains in cardiolipin content bilayers. Ultramicroscopy **107**:943–947.
15. **Epand RM, Epand RF.** 2011. Bacterial membrane lipids in the action of antimicrobial agents. J. Pept. Sci. **17**:298–305.
16. **Epand RM, Epand RF.** 2009. Domains in bacterial membranes and the action of antimicrobial agents. Mol. Biosyst. **5**:580–587.
17. **Fujita KI, Fujita T, Kubo I.** 2008. Antifungal activity of alkanols against *Zygosaccharomyces bailii* and their effects on fungal plasma membrane. Phytother. Res. **22**:1349–1355.
18. **Giocondi MC, et al.** 2010. Surface topography of membrane domains. Biochim. Biophys. Acta **1798**:703–718.
19. **Glover RE, Smith RR, Jones MV, Jackson SK, Rowlands CC.** 1999. An EPR investigation of surfactant action on bacterial membranes. FEMS Microbiol. Lett. **177**:57–62.
20. **Hatzakis NS, et al.** 2009. How curved membranes recruit amphipathic helices and protein anchoring motifs. Nat. Chem. Biol. **5**:835–841.
21. **Hilmarsson H, Kristmundsdóttir T, Thormar H.** 2005. Virucidal activities of medium- and long-chain fatty alcohols, fatty acids and monoglycerides against herpes simplex virus types 1 and 2: comparison at different pH levels. APMIS **113**:58–65.
22. **Huang KC, Ramamurthi KS.** 2010. Macromolecules that prefer their membranes curvy. Mol. Microbiol. **76**:822–832.
23. **Jackson MB, Cronan JE, Jr.** 1978. An estimate of the minimum amount of fluid lipid required for the growth of *Escherichia coli.* Biochim. Biophys. Acta **512**:472–479.
24. **Kabara JJ.** 1984. Antimicrobial agents derived from fatty acids. J. Am. Oil Chem. Soc. **61**:397–403.
25. **Kabara JJ, Swieczkowski DM, Conley AJ, Truant JP.** 1972. Fatty acids and derivatives as antimicrobial agents. Antimicrob. Agents Chemother. **2**:23–28.
26. **Kollanoor A, Vasudevan P, Nair MKM, Hoagland T, Venkitanarayanan K.** 2007. Inactivation of bacterial fish pathogens by medium-chain lipid molecules (caprylic acid, monocaprylin and sodium caprylate). Aquacult. Res. **38**:1293–1300.

27. **Koppelman CM, Den Blaauwen T, Duursma MC, Heeren RMA, Nanninga N.** 2001. *Escherichia coli* minicell membranes are enriched in cardiolipin. J. Bacteriol. **183**:6144–6147.
28. **Mädler B, Binder H, Klose G.** 1998. Compound complex formation in phospholipid membranes induced by a nonionic surfactant of the oligo-(ethylene oxide)-alkyl ether type: a comparative DSC and FTIR study. J. Colloid Interface Sci. **202**:124–138.
29. **Marshall D, Kabara J.** 2005. Medium-chain fatty acids and esters, p 327–360. *In* Antimicrobials in food, 3rd ed. CRC Press, Boca Raton, FL.
30. **Meyer RL, et al.** 2010. Immobilisation of living bacteria for AFM imaging under physiological conditions. Ultramicroscopy **110**:1349–1357.
31. **Mileykovskaya E, Dowhan W.** 2009. Cardiolipin membrane domains in prokaryotes and eukaryotes. Biochim. Biophys. Acta **1788**:2084–2091.
32. **Mortensen NP, et al.** 2009. Effects of colistin on surface ultrastructure and nanomechanics of *Pseudomonas aeruginosa* cells. Langmuir **25**:3728–3733.
33. **Nair MKM, Vasudevan P, Hoagland T, Venkitanarayanan K.** 2004. Inactivation of *Escherichia coli* O157:H7 and *Listeria monocytogenes* in milk by caprylic acid and monocaprylin. Food Microbiol. **21**:611–616.
34. **Nobmann P, Smith A, Dunne J, Henehan G, Bourke P.** 2009. The antimicrobial efficacy and structure activity relationship of novel carbohydrate fatty acid derivatives against *Listeria* spp. and food spoilage microorganisms. Int. J. Food Microbiol. **128**:440–445.
35. **Ocampo J, Afanador N, Vives MJ, Moreno JC, Leidy C.** 2010. The antibacterial activity of phospholipase A2 type IIA is regulated by the cooperative lipid chain melting behavior in *Staphylococcus aureus*. Biochim. Biophys. Acta **1798**:1021–1028.
36. **Perez L, Pinazo A, Garcia MT, Moran MD, Infante MR.** 2004. Monoglyceride surfactants from arginine: synthesis and biological properties. New J. Chem. **28**:1326–1334.
37. **Richter RP, Bérat R, Brisson AR.** 2006. Formation of solid-supported lipid bilayers: an integrated view. Langmuir **22**:3497–3505.
38. **Russell NJ, Gould GW.** 2003. Food preservatives. Kluwer Academic/Plenum Publishers, New York, NY.
39. **Sun CQ, O'Connor CJ, Roberton AM.** 2003. Antibacterial actions of fatty acids and monoglycerides against *Helicobacter pylori*. FEMS Immunol. Med. Microbiol. **36**:9–17.
40. **Sundh M, Svedhem S, Sutherland DS.** 2010. Influence of phase separating lipids on supported lipid bilayer formation at SiO2 surfaces. Phys. Chem. Chem. Phys. **12**:453–460.
41. **Wang LL, Johnson EA.** 1992. Inhibition of *Listeria monocytogenes* by fatty acids and monoglycerides. Appl. Environ. Microbiol. **58**:624–629.